THE JOURNAL OF BIOLOGICAL CHEMISTRY VOL. 287, NO. 51, pp. 42835–42845, December 14, 2012

The Plasma Membrane Sialidase NEU3 Regulates the Malignancy of Renal Carcinoma Cells by Controlling β1 Integrin Internalization and Recycling*[S]

Received for publication, August 3, 2012, and in revised form, November 7, 2012 Published, JBC Papers in Press, November 8, 2012, DOI 10.1074/jbc.M112.407718

Cristina Tringali[‡], Barbara Lupo[‡], Ilaria Silvestri[‡], Nadia Papini[‡], Luigi Anastasia[§¶], Guido Tettamanti[¶], and Bruno Venerando[‡¶1]

From the Departments of [‡]Medical Biotechnology and Translational Medicine and [§]Biomedical Sciences for Health, University of Milan, Segrate, 20090 Milan, Italy and the [¶]IRCCS Policlinico San Donato, San Donato Milanese, 20097 Milan, Italy

Background: NEU3 is involved in ganglioside surface metabolism and is up-regulated in renal carcinoma cells.
Results: NEU3 regulates β1 integrin trafficking and the downstream FAK/AKT pathway, influencing drug resistance and invasive potential.
Conclusion: NEU3 is a key regulator of renal cell carcinoma malignancy.
Significance: NEU3 could be a new target for molecular therapies for renal carcinoma.

The human plasma membrane sialidase NEU3 is a key enzyme in the catabolism of membrane gangliosides, is crucial in the regulation of cell surface processes, and has been demonstrated to be significantly up-regulated in renal cell carcinomas (RCCs). In this report, we show that NEU3 regulates β1 integrin trafficking in RCC cells by controlling β1 integrin recycling to the plasma membrane and controlling activation of the epidermal growth factor receptor (EGFR) and focal adhesion kinase (FAK)/protein kinase B (AKT) signaling. *NEU3* silencing in RCC cells increased the membrane ganglioside content, in particular the GD1a content, and changed the expression of key regulators of the integrin recycling pathway. In addition, *NEU3* silencing up-regulated the Ras-related protein RAB25, which directs internalized integrins to lysosomes, and down-regulated the chloride intracellular channel protein 3 (CLIC3), which induces the recycling of internalized integrins to the plasma membrane. In this manner, *NEU3* silencing enhanced the caveolar endocytosis of β1 integrin, blocked its recycling and reduced its levels at the plasma membrane, and, consequently, inhibited EGFR and FAK/AKT. These events had the following effects on the behavior of RCC cells: they (*a*) decreased drug resistance mediated by the block of autophagy and the induction of apoptosis; (*b*) decreased metastatic potential mediated by down-regulation of the metalloproteinases *MMP1* and *MMP7*; and (*c*) decreased adhesion to collagen and fibronectin. Therefore, our data identify NEU3 as a key regulator of the β1 integrin-recycling pathway and FAK/AKT signaling and demonstrate its crucial role in RCC malignancy.

Renal cell carcinoma (RCC)[2] accounts for ~2–3% of all cancer diagnoses each year, and the incidence of this cancer has been rising steadily. RCC has the highest mortality rate among genitourinary cancers (1) and encompasses many histological subtypes, among which clear cell RCC, also called conventional RCC, is the most common subtype (2). RCC is characterized by a highly angiogenic and invasive phenotype and is highly resistant to radiation or chemotherapy (1). Its molecular signature includes several alterations of the *VHL* gene, the platelet-derived growth factor and epidermal growth factor receptors (PDGFR and EGFR), the phosphatidylinositol-3 kinase (PI3K)/protein kinase B (AKT) pathway (3), integrins (4), and the expression of gangliosides, such as sialic acid-containing glycosphingolipids, which are usually poorly represented in normal kidney tissues (5). In particular, the high content of globo-series gangliosides, particularly monosialosyl galactosylgloboside (MSGG), increases metastatic potential and is inversely correlated with patient survival (6). Moreover, gangliosides that are highly shed by RCCs induce immune cell dysfunction (7). Consistent with the appearance of a distinct repertoire of gangliosides, several crucial enzymatic mechanisms that regulate ganglioside synthesis appear to be deregulated in RCC. β-1,4-GalNAc transferase (β1,4GalNAc-T) (8), α-2,3-sialyltransferase (ST3GalII) (6), and the plasma membrane-associated sialidase, NEU3 (9), have been demonstrated to be altered with regard to mRNA expression and activity in RCC compared with normal kidney tissue. In particular, the sialidase NEU3 has been demonstrated to play an important role in RCC pathogenesis (9). *NEU3* mRNA levels are reported to be significantly higher in RCC than in adjacent non-tumor tissues (9). *NEU3* has been demonstrated to be up-regulated by interleukin-6 (IL-6) and to act in a positive feedback manner on cytokine function by enhancing the PI3K/AKT signaling pathway, which

* This work was supported by MIUR (PRIN 2008) and Fondazione Cariplo (2010-0700) (to B. V.).
[S] This article contains supplemental Table S1.
[1] To whom correspondence should be addressed: Department of Medical Biotechnology and Translational Medicine, University of Milan, via F.lli Cervi 93, Segrate Milan, 20090, Italy. Tel.: +39-(02)-50330361; Fax +39-(02)-50330365; E-mail: bruno.venerando@unimi.it.
[2] The abbreviations used are: RCC, renal cell carcinoma; FAK, focal adhesion kinase; AKT, protein kinase B; EGFR, epidermal growth factor receptor; RAB25, Ras-related protein RAB25; CLIC3, chloride intracellular channel protein 3; MMP, metalloproteinase; PDGFR, platelet-derived growth factor receptor; β-1,4-GalNAc transferase, β-1,4GalNAc-T; α-2,3-sialyltransferase, ST3GalII; PI3K, phosphatidylinositol-3 kinase; MSGG, monosialosyl galactosylgloboside; MβCD, methyl-β-cyclodextrin; CAV1, caveolin 1; SM, sphingomyelin; Gb3, globoside 3; GlcCer, glucosylceramide; LacCer, lactosylceramide; Cer, ceramide; HPTLC, high performance thin layer chromatography.

results in the suppression of apoptosis and the promotion of migration (9). In addition to RCC, the up-regulation of *NEU3* has been observed in other tumor types, including colon, ovarian, prostate cancer, and chronic myeloid leukemia, although the down-regulation of *NEU3* has been observed in acute lymphoblastic leukemia (10–13). Because of its recognition of gangliosides as substrates (14), NEU3 is involved in transmembrane signaling and activates several surface receptors, including EGFR and β4 integrin, which are involved in oncogenesis (15, 16).

We sought to better elucidate the role of *NEU3* up-regulation in RCC. We stably silenced *NEU3* in a primary clear cell RCC line and in undifferentiated papillary RCC cell line. Our results further corroborated the oncogenic activation induced by this enzyme and demonstrated that in *NEU3*-silenced cells there was an increase in GD1a content, which had the following consequences: (*a*) a change in cellular behavior, particularly decreased drug resistance, invasive potential, and adhesion; (*b*) at the molecular level, impaired β1 integrin recycling to the plasma membrane, and partially inhibited the focal adhesion kinase (FAK)/AKT signaling.

EXPERIMENTAL PROCEDURES

Cell Culture and Stable Silencing of NEU3 in RCC Cells—Human primary RCC cell lines were established from surgical specimens and were kindly provided by Dr. Protti (S. Raffaele Hospital, Milan). The CA-TC cell line was chosen from this panel because it carries lesions and features that are typical of clear cell carcinoma. By contrast, GR-TC cells are from an undifferentiated papillary RCC. The CA-TC and GR-TC cells were cultured in RPMI 1640 medium supplemented with 10% (v/v) FBS and 2 mM glutamine (Sigma-Aldrich). To stably silence *NEU3*, a short hairpin targeting the human *NEU3* gene sequence was designed with the BlockiT RNAi Designer software (Invitrogen, Grand Island, NY). The CA-TC and GR-TC cells were infected at an MOI of 5 according to the manufacturer's instructions. The infected clones were isolated after selection with 600 μg/ml zeocin. To deplete the cholesterol and block the caveola-mediated endocytosis, 1×10^6 mock-treated and *NEU3*-silenced CA-TC cells were treated with 1 mM methyl-β-cyclodextrin (MβCD) (Sigma-Aldrich) for 3 h at 37 °C. AKT was inhibited in the mock CA-TC cells by adding 10 μM LY294002 to the cell culture medium for 24 h.

GD1a Enrichment of CA-TC Cells—To enrich for GD1a content, the CA-TC cells were cultivated in Optimem I medium (Invitrogen) containing 50 μM GD1a that was purified from a total ganglioside mixture extracted from bovine brain (17). The cells were incubated for 48 h at 37 °C.

Real-time RT-PCR—Real-time PCR was performed as previously reported (13). Primer sequences are shown in supplemental Table S1.

Cell Apoptosis and Autophagy Assays—To evaluate drug resistance, 2×10^5 mock and *NEU3*-silenced CA-TC and GR-TC cells were treated with 20 μM etoposide for 24 h. Cell viability was assessed after staining with SYTOX Green nucleic acid stain (Invitrogen). Caspase-3 activation was determined by Western blotting with an antibody recognizing the cleaved fragment of caspase-3 (Cell Signaling, Danvers, MA). Autophagy was determined by staining etoposide-treated cells with 1 μg/ml acridine orange (Sigma-Aldrich) for 15 min and then obtaining microphotographs using an inverted fluorescence microscope (IX50 Olympus). LC3B-II conversion was quantified by Western blotting using an anti-LC3B antibody (Sigma-Aldrich).

Sialidase Activity Assay—The sialidase activity that was present in the particulate fraction of the mock and *NEU3*-silenced CA-TC and GR-TC cells was assayed using [^{3}H]GD1a at pH 3.8 as previously reported (13). One unit of sialidase activity is defined as the amount of enzyme liberating 1 μmol product per min.

Cell Invasiveness Assay—The invasive potential of 2×10^5 mock and *NEU3*-silenced CA-TC cells was assayed *in vitro* using a Matrigel Invasion Chamber according to the manufacturer's instructions (BD Biosciences, Franklin Lakes, NJ).

Cell Adhesion Assay—Mock and *NEU3*-silenced CA-TC cells (2×10^5) were resuspended in serum-free RPMI 1640 medium and plated in 6-well plates coated with fibronectin or collagen type I (Sigma-Aldrich). The cells were incubated at 37 °C for 30 min. The cell culture plates were washed twice with phosphate-buffered saline (PBS) to remove any unbound cells, fixed with 70% ethanol for 20 min at 4 °C, stained with 0.1% crystal violet (Sigma-Aldrich) at room temperature for 20 min, and washed twice with water. The crystal violet was eluted with 0.1% (v/v) acetic acid, and cell adhesion was determined at 550 nm on a Victor microplate reader (Perkin Elmer, Waltham, MA).

Zymography—Serum-free conditioned medium was collected from mock and *NEU3*-silenced CA-TC cells and loaded on 10% polyacrylamide gel containing 1 mg/ml gelatin or 0.5 mg/ml type I collagen. After electrophoresis, the gels were incubated in 2.5% (v/v) Triton X-100 for 30 min, at room temperature, and in 50 mM Tris/HCl, 0.2 M NaCl, 5 mM $CaCl_2$, 0.02% (v/v) Brij 35, at 37 °C for 18 h. Then, the gels were stained with 0.5 (w/v) Coomassie Brilliant Blue G and destained. Gelatinolytic activities were quantified using the Quantity One software (Bio-Rad).

Western Blot—Proteins (25 μg) were separated on 10% SDS-PAGE, and transferred onto PVDF membrane. The following antibodies were used for the assays: anti-NEU3, anti-AKT, anti-FAK, anti-SRC, anti-β-actin (Santa Cruz Biotechnology), anti-P-AKT (Ser-473), anti-EGFR, anti-P-EGFR (Tyr-1148), anti-phospho-SRC (Tyr-416), anti-cleaved caspase 3 (Cell Signaling), anti-BCL-2 (Sigma-Aldrich), anti-CAV1, anti-β1 integrin, anti-P-FAK (Tyr-397) (BD Biosciences). Blots were quantified using GS-700 calibrated densitometer, and the Quantity One software (Bio-Rad).

Biotin Internalization and Recycling Assays—Mock and *NEU3*-silenced CA-TC cells (8×10^5) were washed with PBS and incubated with 0.2 mg/ml Sulfo-NHS-SS-Biotin (Pierce) for 30 min at 4 °C. The internalization and recycling assays were performed as described by Steinberg *et al.* (18).

Metabolic Labeling of Cell Sphingolipids—[^{3}H]sphingosine (Perkin Elmer) cell labeling was performed as previously described (13).

Statistical Analyses—The values are presented as the mean ± S.D. The statistical analyses were performed using Student's *t*

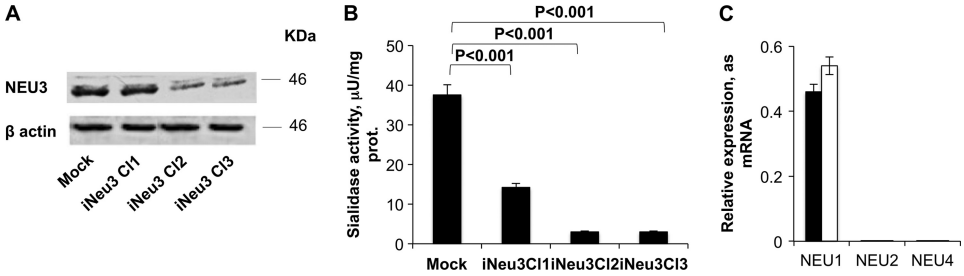

FIGURE 1. **Silencing of NEU3 in CA-TC cells.** *A*, NEU3 protein level was assessed by Western blot analysis of three selected clones. *β*-actin was used as the loading control. The blot is representative of four independent experiments. *B*, sialidase activity of mock and *NEU3*-silenced clones assayed with [^{3}H] GD1a at pH 3.8. *C*, *NEU1* sialidase mRNA expression assessed by real time PCR in mock (*black bar*) and iNeu3Cl2 (*white bar*) cells. The values are the mean ± S.D. of four independent experiments.

test, and the mock data were compared with the data from the *NEU3*-silenced clone.

RESULTS

NEU3 Silencing in RCC CA-TC Cells—The clear cell carcinoma cell line CA-TC was chosen for this study from a panel of RCC primary cells because it is representative of the most common RCC subtype. After infection of the CA-TC cells with a lentiviral vector containing the short hairpin targeting the *NEU3* gene, three clones were selected with zeocin. NEU3 showed a decreased protein content of 10–90% ($p < 0.01$) (Fig. 1*A*) and a decreased catalytic activity toward the ganglioside GD1a of 62–92% (Fig. 1*B*). In particular, clone 2, referred to as iNeu3Cl2, showed the lowest NEU3 expression, which was quantified as a 90% lower protein content and a 92% lower catalytic activity than the mock cells (Fig. 1, *A* and *B*). After *NEU3* silencing, in each clone, the expression of the lysosomal sialidase *NEU1* did not significantly change, whereas the *NEU2* and *NEU4* mRNA continued to be undetectable, similar to the findings for the mock cells (Fig. 1*C*). iNeu3Cl2 was primarily used for the assays described below. iNeu3Cl1 gave similar results to those obtained with the mock cells, whereas iNeu3Cl3 showed a similar behavior to the iNeu3Cl2 clone. For several of the experiments, we reported the results obtained for all the clones.

NEU3 Silencing Alters the Glycosphingolipid Pattern of CA-TC Cells—Because gangliosides are the preferred substrates of NEU3 (14, 19), we postulated that *NEU3* silencing could alter the composition of the glycosphingolipids present in CA-TC cells. The sphingolipid pattern was evaluated by metabolic labeling with [3-^{3}H]sphingosine. After a 2 h pulse followed by a 24 h chase, a metabolic steady state was obtained. As expected, the ganglio- and globo-ganglioside profile of iNeu3Cl2 cells was different from that of mock cells. GD1a, GM2, and GM3 content underwent a 188, 37, and 88% increase, respectively, and MSGG decreased by 61% (Fig. 2, *A* and *B*). Among the neutral sphingolipids, sphingomyelin (SM) content decreased by 26%, and the content of globoside 3 (Gb3), which is the biosynthetic precursor of MSGG, decreased by 29%; by contrast, glucosylceramide (GlcCer) content increased by 197% (Fig. 2, *C* and *D*). The same alterations were also observed in the iNeu3Cl3 cells (data not shown). Notably, *NEU3* silencing induced significant modifications in the expression of pivotal enzymes that regulate the synthesis of CA-TC cell glycosphingolipids. In particular, *α*-1,4-galactosyltransferase (*A4GALT*), which catalyzes the synthesis of Gb3 from lactosylceramide, showed a 57% decrease in mRNA content, whereas GM3 synthase, which uses lactosylceramide for the synthesis of GM3, showed a 293% increase in mRNA content (Fig. 2*E*). Additionally, GM2 synthase mRNA increased by 57% (Fig. 2*E*). These data provide a better understanding of the mechanisms that lead to decreased Gb3 and MSGG levels and increased ganglio-ganglioside levels.

NEU3 Silencing Reduces Resistance to Drugs in CA-TC Cells—Because gangliosides are closely involved in the control of many cellular processes and carcinogenesis (20), we hypothesized that changes induced by *NEU3* silencing could trigger important effects on CA-TC cell behavior and malignancy. In fact, consistent with data from other cancer types (13) and CA-TC cells, *NEU3* silencing significantly modified the configuration of the apoptotic machinery. *NEU3* silencing increased the mRNA expression of the pro-apoptotic molecules *BAD* (105%) and *BAX* (104%) and decreased the expression of the anti-apoptotic protein *BCL-2* (20%). In contrast to this trend, *BCL-XL* mRNA underwent a 30% increase (Fig. 3*A*). In particular, BCL-2 protein expression was investigated in all of the isolated clones. A 48% ($p < 0.05$) and 20% decrease ($p < 0.05$) in BCL-2 protein expression was observed in the iNeu3Cl2 and iNeu3Cl3 cells, respectively (Fig. 3*B*). This new molecular profile changed the cellular response to 24 h etoposide treatment. Etoposide induced the death of 40% of the mock cells and 60% of the iNeu3Cl2 cells; therefore, the drug sensitivity of the iNeu3Cl2 cells increased by 50% (Fig. 3*C*). To investigate the mechanisms of cell death that were induced by etoposide, we searched for the expression of typical markers of autophagy and apoptosis. First, acridine orange vital staining was used to visualize the formation of acidic autophagolysosomes in the non-treated and etoposide-treated mock and iNeu3Cl2 cells. As shown in Fig. 3*D*, in the absence of etoposide, autophagolysosomes were present in the mock cells, and etoposide treatment further increased the number of autophagolysosomes (Fig. 3*D*). By contrast, autophagolysosomes were not detected in the non-treated and etoposide-treated iNeu3Cl2 cells (Fig. 3*D*). Consistent with this observation, the non-treated mock cells showed a high activation of the LC3B-I protein, which precedes the formation of LC3B-II and is characteristic of the initiation of the autophagic pathway. Etoposide treatment significantly increased the amount of LC3B-II in the mock cells (3.15-fold; $p < 0.01$) but not the Neu3Cl2 cells (Fig. 3*E*). To investigate

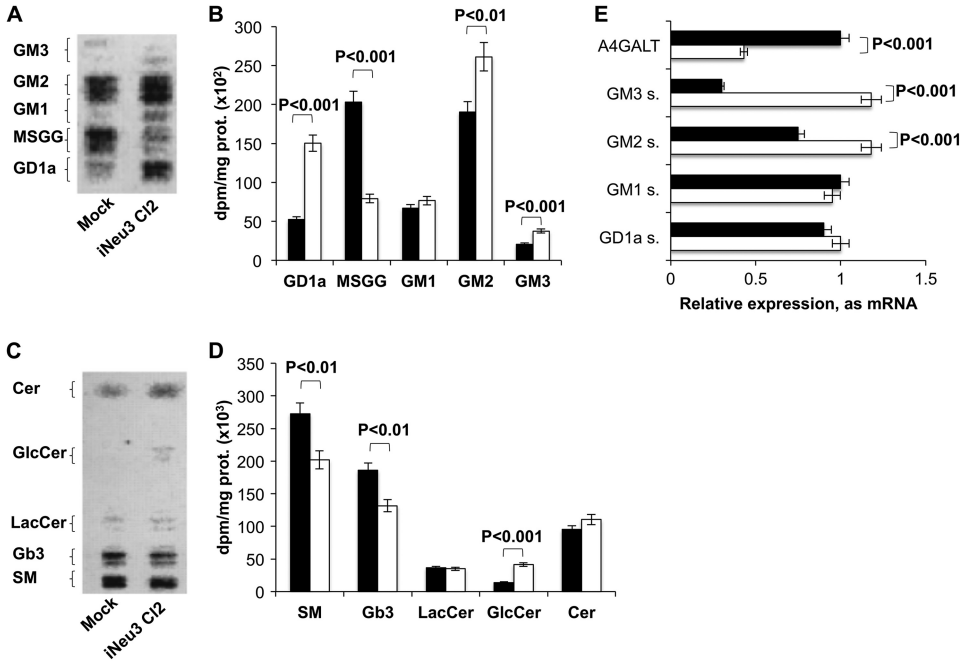

FIGURE 2. **Effect of NEU3 silencing on CA-TC cell sphingolipid pattern.** *A*, HPTLC separation of mock and iNeu3Cl2 cell gangliosides. The doublets are due to the heterogeneity of the ceramide moiety. Solvent system: chloroform/methanol/0.2% aqueous $CaCl_2$ 60:40:9 (v/v). The image was acquired by radiochromatoscanning (Beta Imager 2000). *B*, ganglioside content of mock (*black bar*) and iNeu3Cl2 (*white bar*) cells. The values are the mean ± S.D. of five independent experiments. *C*, HPTLC separation of mock and iNeu3Cl2 cell neutral sphingolipids. Solvent system: chloroform/methanol/H_2O 55:20:3 (v/v). The image was acquired by radiochromatoscanning (Beta Imager 2000). *D*, neutral sphingolipid content of mock (*black bar*) and iNeu3Cl2 (*white bar*) cells. The values are the mean ± S.D. of five independent experiments. *E*, real time PCR analysis of the mRNA expression of the primary enzymes involved in ganglioside synthesis in mock (*black bar*) and iNeu3Cl2 (*white bar*) cells. The values are the mean ± S.D. of three independent experiments.

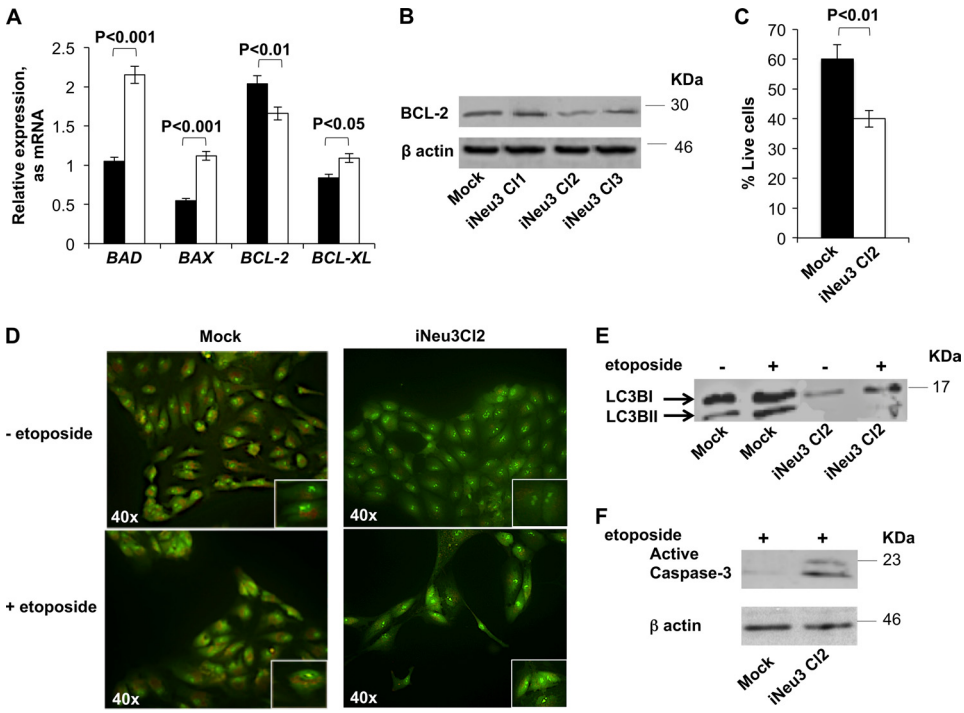

FIGURE 3. **Effects of NEU3 silencing on CA-TC cell drug resistance.** *A*, real time PCR analysis of mRNA levels of members of the BCL-2 family in mock (*black bar*) and iNeu3Cl2 (*white bar*) cells. The values are the mean ± S.D. of five independent experiments. *B*, BCL-2 protein content assessed by Western blot in mock and *NEU3*-silenced clones. β-Actin was used as the loading control. The values are the mean ± S.D. of five independent experiments. *C*, mock (*black bar*) and iNeu3Cl2 (*white bar*) cell viability was determined with SYTOX staining after etoposide treatment. The values are the mean ± S.D. of five independent experiments. *D*, detection of acidic vesicular organelles in etoposide-treated mock and iNeu3Cl2 cells with acridine orange staining. The cells were examined by fluorescence microscopy. Representative images from three independent experiments were shown. Original magnification ×40 (Olympus Ix50). *E*, Western blot analysis of LC3B proteins in mock and iNeu3Cl2 cells after etoposide treatment. The blot is representative of four independent experiments. *F*, caspase 3 activation was determined by evaluation of the corresponding cleavage fragment in mock and iNeu3Cl2 cells after treatment with etoposide. β-Actin was used as the loading control. The blot is representative of four independent experiments.

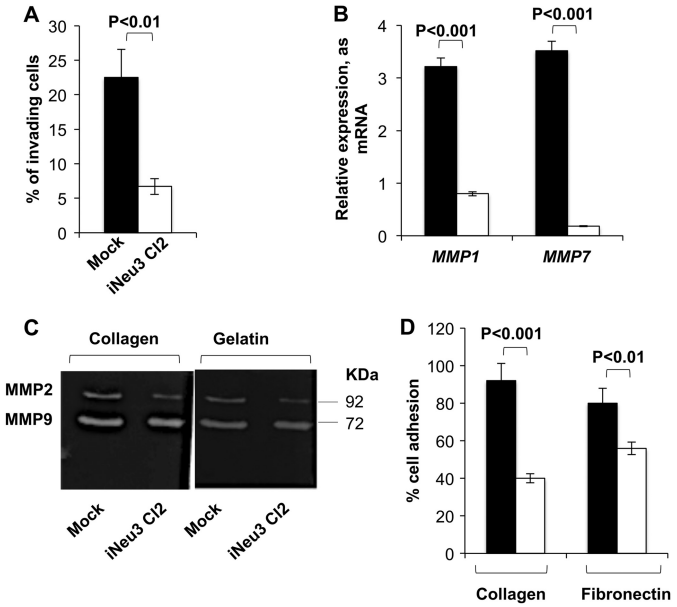

FIGURE 4. **Effects of NEU3 silencing on CA-TC cell invasion and adhesion potential.** *A*, matrigel invasion assay of mock (*black bar*) and iNeu3Cl2 (*white bar*) cells. The values are the mean ± S.D. of five independent experiments. *B*, real time PCR analysis of *MMP1* and *MMP7* mRNA expression in mock (*black bar*) and iNeu3Cl2 (*white bar*) cells. The values are the mean ± S.D. of five independent experiments. *C*, representative collagen and gelatin zymograms of conditioned medium collected from mock and iNeu3Cl2 cells. *D*, mock (*black bar*) and iNeu3Cl2 (*white bar*) cell adhesion assay to collagen type I-coated wells and fibronectin-coated wells. The values are the mean ± S.D. of five independent experiments.

apoptosis, we evaluated caspase-3 activation by detecting the presence of the corresponding cleaved fragment. With regard to caspase-3 activation, etoposide had no effect on the mock cells; however, it was effective on the iNeu3Cl2 cells as demonstrated by the appearance of the 17–19 kDa caspase-3 fragment ($p < 0.001$) (Fig. 3*F*).

NEU3 Silencing Reduces the Invasive Potential of CA-TC Cells and Induces the Down-regulation of the Matrix Metalloproteinase-1 (MMP1) and Metalloproteinase-7 (MMP7) Genes—The second modification affecting the malignant behavior of *NEU3*-silenced CA-TC cells was linked to invasive potential. *NEU3* silencing reduced the invasiveness of CA-TC cells by 70.2% as assessed with Matrigel-coated filters (invading mock cells after 24 h, 22.5%; invading iNeu3Cl2 cells after 24 h, 6.7%) (Fig. 4*A*). It is well known that MMPs play a central role in regulating tumor cell invasion and in remodeling the stromal microenvironment (21). To investigate whether NEU3 affected RCC cell invasion by modulating the expression/activity of MMPs, we determined the gene expression of the primary MMPs that act in RCC. *MMP1* and *MMP7* expression was reduced by 75 and 95%, respectively, in the iNeu3Cl2 cells compared with the mock cells (Fig. 4*B*). Although the gene expression of *MMP9* and *MMP2* remained unchanged after *NEU3* silencing (data not shown), in zymographic assays, the MMP2 and MMP9 collagenolytic activity decreased by 35 and 15%, respectively ($p < 0.05$), and the gelatinolytic activity decreased by 25 and 17%, respectively ($p < 0.05$) (Fig. 4*C*). This evidence could be directly linked to the down-regulation of *MMP7* because MMP7 enzymatically activates MMP9 and MMP2 (22). In addition, iNeu3Cl2 cells showed less adhesion to type I collagen (−56.5%) and fibronectin (−30%) compared with mock cells (Fig. 4*D*).

NEU3 Silencing Alters the Recycling Pattern of β1 Integrin to the Plasma Membrane in CA-TC Cells—To clarify the molecular mechanisms that are regulated by NEU3 in CA-TC cells, we assessed the surface content/activation of key signaling proteins. In the iNeu3Cl2 and iNeu3Cl3 cells, we detected a decrease in the plasma membrane levels of caveolin 1 (CAV1) by 67 and 76%, respectively, and of β1 integrin by 40 and 30%, respectively ($p < 0.01$) (Fig. 5*A*). The mRNA expression of both β1 integrin and *CAV1* was unchanged (data not shown). Therefore, these data indicated that the synthesis of β1 integrin and CAV1 was not impaired in the *NEU3*-silenced clones. Because CAV1 is the main component of caveolae and is a key regulator of the endocytic route and internalization of integrins (23), we hypothesized that an alteration of endocytosis via caveolae could occur after *NEU3* silencing. Additionally, this could be related to the decrease in β1 integrin at the plasma membrane. To test this hypothesis, we treated mock and iNeu3Cl2 cells with the cholesterol-depleting agent, MβCD, to disrupt caveolae and block caveola-mediated endocytosis. As shown in Fig. 5*B*, after MβCD treatment, the amount of β1 integrin localized to the cell surface of the iNeu3Cl2 cells was higher than on the mock cell surface (+58%; $p < 0.05$). This is the opposite of that observed in the absence of MβCD. To directly investigate the internalization process of β1 integrin in the mock and iNeu3Cl2 cells, we used a biotin internalization assay. The internalized β1 integrin was quantified by calculating the percentage of biotinylated/internalized β1 integrin in relation to the total amount of β1 integrin. We demonstrated that the internalization of β1 integrin occurred more rapidly in the iNeu3Cl2 cells than in the mock cells (+125% after 2 min; +48% after 10 min, respectively) (Fig. 5*C*). Further demonstrating the occurrence of more rapid caveolar endocytosis, SRC kinases that are crucial for this process (24) were more abundant (+102%; $p < 0.01$) and active (+222%; $p < 0.01$) in the iNeu3Cl2 cells in comparison to mock cells (Fig. 5*D*). Moreover, the fate of the internalized β1 integrin was different in the mock and iNeu3Cl2 cells. The recycling of β1 integrin from the endosomes and perinuclear compartment was monitored using a pulse-chase technique. In the mock cells, 70% of the internalized β1 integrin returned to the plasma membrane within 15 min *versus* 15% in the iNeu3Cl2 cells (Fig. 5*E*). By contrast, in the iNeu3Cl2 cells, 40% of the β1 integrin appeared to be degraded because after a 30 min incubation at 37 °C, the amount of total β1 integrin decreased by 40%. Conversely, no change in the total amount of β1 integrin was detected in the mock cells (Fig. 5*F*). To identify a molecular explanation for these results, we evaluated the mRNA expression of two proteins, the Ras-related protein RAB25 and the chloride intracellular channel protein 3 (CLIC3), which were previously reported to regulate the fate of internalized β1 integrin (25). In cancer cells that lack CLIC3, routes active integrins to lysosomes where they are degraded. Conversely, when CLIC3 is up-regulated, lysosomally routed active integrins return to the plasma membrane, enabling their continued signaling. As shown in Fig. 5*G*, in the mock cells, the expression of *CLIC3* was higher than *RAB25* (+400%), whereas in the iNeu3Cl2 cells, the

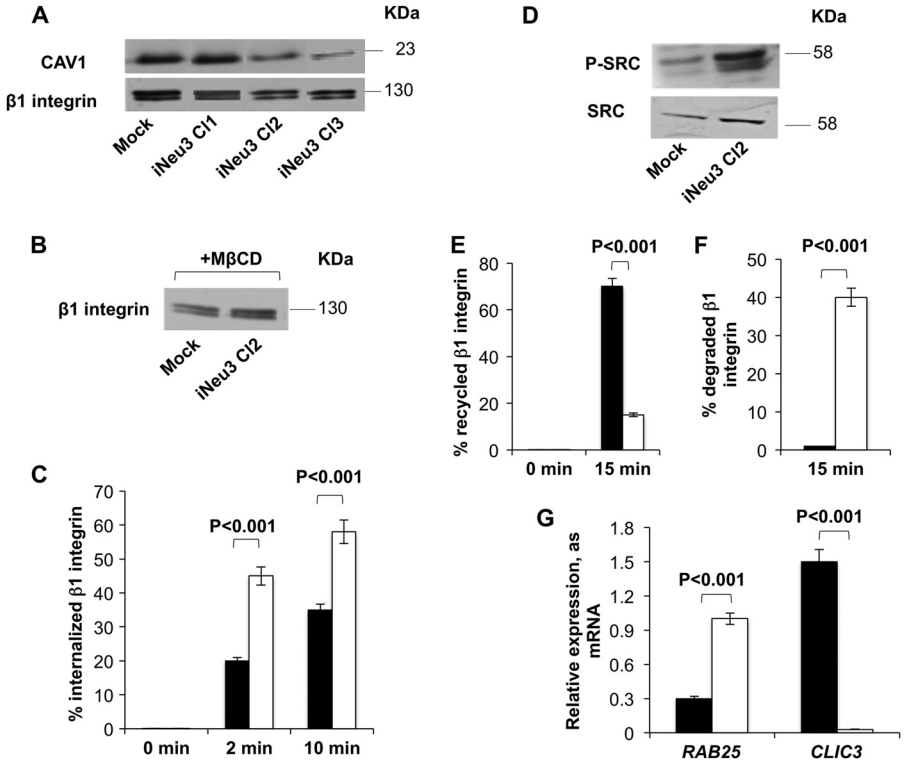

FIGURE 5. **Modification of β1 integrin trafficking induced by NEU3 silencing in CA-TC cells.** *A*, Western blot image of mock and *NEU3*-silenced clone cell membrane fractions probed with anti-CAV1 and anti-β1 integrin antibodies. An equal amount of protein was loaded in each lane. The blots are representative of five independent experiments. *B*, Western blot analysis of membrane β1 integrin content in mock and iNeu3Cl2 cells after MβCD treatment. An equal amount of protein was loaded in each lane. The blots are representative of four independent experiments. *C*, β1 integrin internalization in mock (*black bar*) and iNeu3Cl2 (*white bar*) cells as determined with biotin internalization assays. The values are the mean ± S.D. of five independent experiments. *D*, Western blot image of mock and iNeu3Cl2 cell lysates probed with anti-SRC and anti-P-SRC antibodies. The blots are representative of four independent experiments. *E*, β1 integrin recycling in mock (*black bar*) and iNeu3Cl2 (*white bar*) cells as determined with biotin recycling assays. The values are the mean ± S.D. of five independent experiments. *F*, β1 integrin degradation in mock (*black bar*) and iNeu3Cl2 (*white bar*) cells determined by calculating the percentage of total biotinylated β1 integrin recovered after 30 min at 37 °C relative to the total starting β1 integrin. The values are the mean ± S.D. of five independent experiments. *G*, real time PCR analysis of *RAB25* and *CLIC3* mRNA expression in mock (*black bar*) and iNeu3Cl2 (*white bar*) cells. The values are the mean ± S.D. of four independent experiments.

RAB25 mRNA increased (+233%) and *CLIC3* was unexpressed compared with the mock cells.

NEU3 Silencing Inhibits the FAK/AKT and EGFR Signaling Pathways in CA-TC Cells—Based on the previous results, we analyzed the primary intracellular signaling pathways associated with β1 integrin. In the iNeu3Cl2 cells, there was a significant down-regulation of FAK signaling as demonstrated by a decrease in the phosphorylated/active form (60%; $p < 0.01$) (Fig. 6*A*). It is well known that FAK is an upstream regulator of the PI3K/AKT signaling pathway (26). Therefore, to assess whether this interaction between the FAK and PI3K/AKT pathways occurs in the CA-TC cells, we evaluated the inhibition of AKT and found a decrease in the phosphorylated/active form (90%, $p < 0.01$) in iNeu3Cl2 cells (Fig. 6*A*). Moreover, the activation/phosphorylation of EGFR was also decreased in the iNeu3Cl2 cells (78%; $p < 0.01$), whereas the membrane content of EGFR remained unchanged ($p < 0.01$) (Fig. 6*B*). Cooperative signaling between integrins and growth factor receptors has been demonstrated previously (27). The down-regulation of AKT that was induced by *NEU3* silencing was demonstrated to be the main factor that was responsible for the effects observed after *NEU3* silencing regarding the autophagy/apoptosis shift and the reduction in invasive potential. In fact, the inhibition of AKT signaling in the mock cells obtained by treatment with the inhibitor LY294002 for 24 h (Fig. 6*C*) led to a decrease in *BCL-2*, *MMP1*, and *MMP7* mRNA expression by 36, 37, and 50%, respectively (Fig. 6*D*).

GD1a Enrichment on the CA-TC Cell Plasma Membrane Down-regulates β1 Integrin Content and Impairs the FAK/AKT Signaling Pathway—Among the modifications to ganglioside patterns that were induced by *NEU3* silencing (Fig. 1*A*), the increase in GD1a content could be a direct effect of the catabolic block caused by the lack of NEU3. To investigate the effects of an increased abundance of GD1a on the CA-TC cell plasma membrane, the mock cells were incubated with 50 μM GD1a for 48 h. After this treatment, the overall effects that were observed were similar to those observed after *NEU3* silencing. *CAV1* was significantly down-regulated (40%; $p < 0.01$), and β1 integrin content on the cell surface also decreased (27%; $p < 0.05$) (Fig. 7*A*). Confirming a modification to β1 integrin trafficking after GD1a incorporation, *RAB25* expression increased by 100%, whereas *CLIC3* expression decreased by 80% (Fig. 7*B*). Therefore, the same downstream modifications of cell signaling that were observed in the *NEU3*-silenced cells occurred in the GD1a-treated mock cells, and FAK activation was decreased by 60% and AKT activation was entirely inhibited (Fig. 7*C*). Additionally, the expression of *BCL2* and *MMP7* mRNA decreased by 55.4 and 29%, respectively (Fig. 7*D*). Fig. 7*E* summarizes the

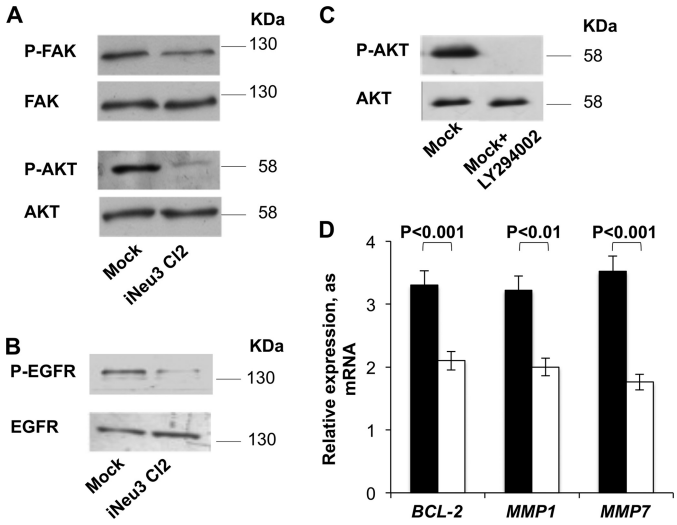

FIGURE 6. **Signaling pathways altered by NEU3 silencing in CA-TC cells.** *A*, Western blot image of total mock and iNeu3Cl2 cell lysates probed with anti-P-FAK, anti-FAK, anti-P-AKT, and anti-AKT antibodies. *B*, Western blot image of mock and iNeu3Cl2 cell membrane fractions probed with anti-P-EGFR and anti-EGFR antibodies. The blots are representative of five independent experiments. *C*, AKT activation in mock cells after 10 μM LY294002 treatment for 24 h. The blot is representative of three independent experiments. *D*, effects of 10 μM LY294002 treatment on the mRNA expression of *BCL-2*, *MMP-1*, and *MMP-7* in mock cells. Non-treated mock cells: *black bar*; LY294002-treated mock cells: *white bar*. The values are the mean ± S.D. of four independent experiments.

molecular mechanisms that were induced by the increase in GD1a after *NEU3* silencing in CA-TC cells.

NEU3 Silencing Alters the Malignant Behavior of Undifferentiated Papillary RCC Cells—To determine whether the effects observed after *NEU3* silencing could be related to the RCC cell type, we silenced the enzyme in an undifferentiated papillary RCC cell line, GR-TC (silencing degree: −80% protein content). Membrane sialidase activity of GR-TC before and after NEU3 silencing is shown in Fig. 8*A*. The ganglioside profile of GR-TC mock cells (GR-mock) was very different from that of CA-TC cells (Fig. 8, *B* and *C*). This observation is not surprising because of the histological dissimilarity between the two cell lines. In the *NEU3*-silenced GR-TC cells (GR-iNeu3), only GD1a was increased (93%) (Fig. 8, *B* and *C*). Among the neutral sphingolipids, Gb3 decreased by 44% (Fig. 8, *D* and *E*), similar to the *NEU3*-silenced CA-TC cells. Moreover, in the GR-iNeu3 cells, we observed similar molecular and behavioral changes to those observed in the *NEU3*-silenced CA-TC cells. In particular, the surface content of β1 integrin decreased by 60% ($p < 0.01$) (Fig. 9*A*). After etoposide treatment, the mortality of the GR-iNeu3 cells increased by 47% (Fig. 9*B*), whereas the GR-mock cells displayed increased autophagy (Fig. 9*C*). Additionally, the expression of MMP1 and MMP7 decreased by 44 and 48%, respectively, in the GR-iNeu3 cells (Fig. 9*D*).

DISCUSSION

Through studying the pathogenesis of RCC, it is becoming clear how alterations in specific signaling pathways make RCC tumors lethal and resistant to therapy (28). In particular, the PI3K/AKT pathway is constitutively active and is responsible for cell growth and survival (29). The up-regulation of the plasma membrane sialidase *NEU3* in RCC has previously been demonstrated to be indirectly involved in altering PI3K/AKT signaling through hyper-activation of the IL-6 pathway (9). Our results further demonstrated that *NEU3* is intrinsically linked to RCC cell deregulation and is directly involved in PI3/AKT activation in an IL-6 independent manner. Our results also demonstrated that through the modulation of ganglioside and globoside content, NEU3 alters β1 integrin trafficking in RCC cells. *NEU3* silencing, which was performed in an RCC cell line that was representative of clear cell carcinoma, drastically modified the sphingolipid pattern. The control of GD1a content seemed to be crucial for RCC cell malignancy, and its increase as a consequence of *NEU3* silencing or after exogenous GD1a incorporation drastically changed the functional activity of the specialized areas of the plasma membrane known as caveolae, where NEU3 has been previously shown to localize (30). These events critically impaired the recycling of β1 integrins, which are closely involved in metastasis, cell growth and survival (27, 31, 32). The ability of gangliosides, including GD1a, to increase caveolar endocytosis has previously been demonstrated (33) and seems to be linked to modifications of the membrane environment, such as cholesterol packing or the induction of CAV1 phosphorylation (24). Therefore, *NEU3* silencing increased the caveolar endocytosis rate via an increased activation of SRC kinases and led to a more rapid internalization of β1 integrins. Notably, the fate of internalized β1 integrins was significantly reprogrammed after *NEU3* silencing. In the mock cells, the internalized β1 integrin was rapidly recycled to the plasma membrane; by contrast, in the *NEU3*-silenced cells, it was sorted toward lysosomes. The differential sorting of caveosomes appeared to be mediated by the up-regulation of *RAB25* and the parallel down-regulation of *CLIC3*. As a result of these events, in the *NEU3*-silenced cells, the concentration of β1 integrin on the plasma membrane was significantly decreased and its associated signaling, which drives tumor progression, was reduced. First, EGFR activation decreased. Cooperative signaling between integrins and growth factor receptors has been demonstrated previously (27). In addition, it could be hypothesized that the increase in GM3 and the decrease in globoside content could work together to reduce EGFR activation (15, 34). Second, the down-regulation of β1 integrin affected the phosphorylation/activation of FAK. FAK colocalizes with integrins and acts as an early sensor of signaling to directly stimulate tumor progression (35) or activate PI3K/AKT (26). Consistent with this view, the down-regulation of FAK was associated with a markedly reduced AKT activation in the *NEU3*-silenced cells. All of these events are schematically depicted in Fig. 7*E*. In addition to the increase in GD1a and GM3 content, *NEU3* silencing induced modifications of the expression of other enzymes involved in sphingolipid synthesis. These events radically altered the balance of sphingolipid synthesis by enhancing the production of ganglio-series gangliosides to the detriment of globo-series gangliosides, in particular MSGG. The increase in globo-series ganglioside content is a process that is intrinsically connected to RCC progression (36). In particular, MSGG is usually absent in healthy renal tissues and is associated with the metastatic potential of RCC (6). The induction of GM3 enrichment on the plasma membrane has been previously demonstrated to cause a concomitant decrease

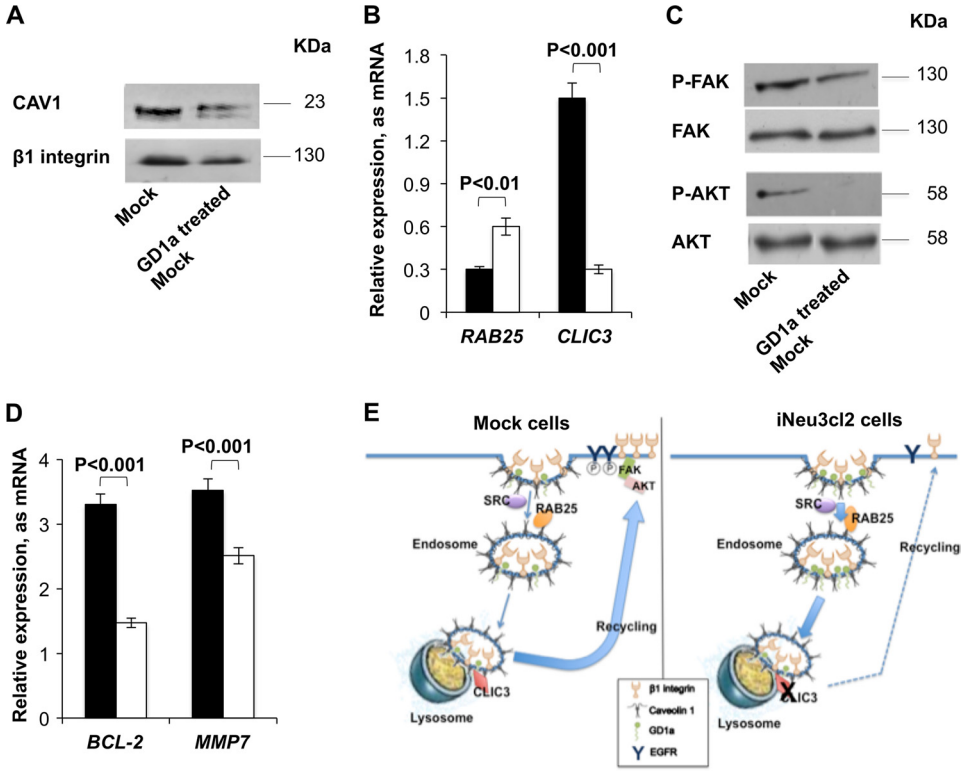

FIGURE 7. **GD1a involvement in the molecular effects induced by NEU3 silencing.** *A*, Western blot image of mock and 50 μM GD1a-treated mock cell membrane fractions probed with anti-CAV1 and anti-β1 integrin antibodies. An equal amount of protein was loaded in each lane. The blots are representative of three independent experiments. *B*, real time PCR analysis of *RAB25* and *CLIC3* mRNA expression in mock (*black bar*) and 50 μM GD1a-treated mock (*white bar*) cells. The values are the mean ± S.D. of three independent experiments. *C*, Western blot image of total mock and 50 μM GD1a-treated mock cell lysates probed with anti-P-FAK, anti-FAK, anti-P-AKT, and anti-AKT antibodies. The blots are representative of three independent experiments. *D*, real time PCR analysis of *BCL-2* and *MMP7* mRNA expression in mock (*black bar*) and 50 μM GD1a-treated mock (*white bar*) cells. The values are the mean ± S.D. of three independent experiments. *E*, schematic image of β1 integrin trafficking in mock and iNeu3Cl2 cells.

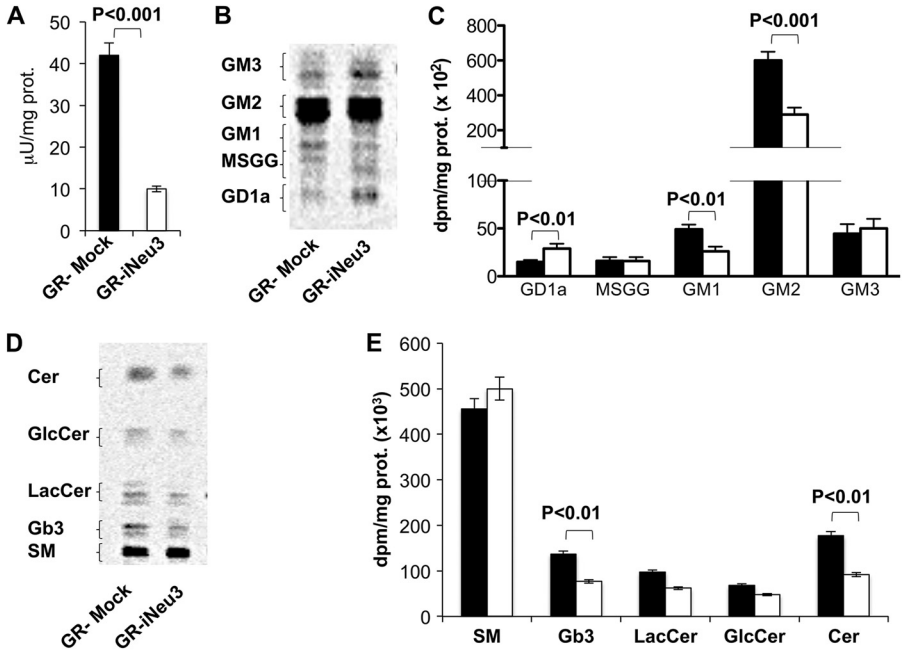

FIGURE 8. **Effect of NEU3 silencing on GR-TC cell sphingolipid pattern.** *A*, sialidase activity of mock and GR-iNeu3 cells assayed with [^{3}H]GD1a at pH 3.8. *B*, HPTLC separation of GR- mock and GR-iNeu3 cell gangliosides. Doublets are due to the heterogeneity of the ceramide moiety. Solvent system: chloroform/methanol/0.2% aqueous $CaCl_2$ 60:40:9 (v/v). Image acquired by radiochromatoscanning (Beta Imager 2000). *C*, ganglioside content of GR-mock (*black bar*) and GR-iNeu3 (*white bar*) cells. Values are the mean ± S.D. of three independent experiments. *D*, HPTLC separation of GR-mock and GR-iNeu3 cell neutral sphingolipids. Solvent system: chloroform/methanol/H_2O 55:20:3 (v/v). Image acquired by radiochromatoscanning (Beta Imager 2000). *E*, neutral sphingolipid content of GR-mock (*black bar*) and GR-iNeu3 (*white bar*) cells. Values are the mean ± S.D. of three independent experiments.

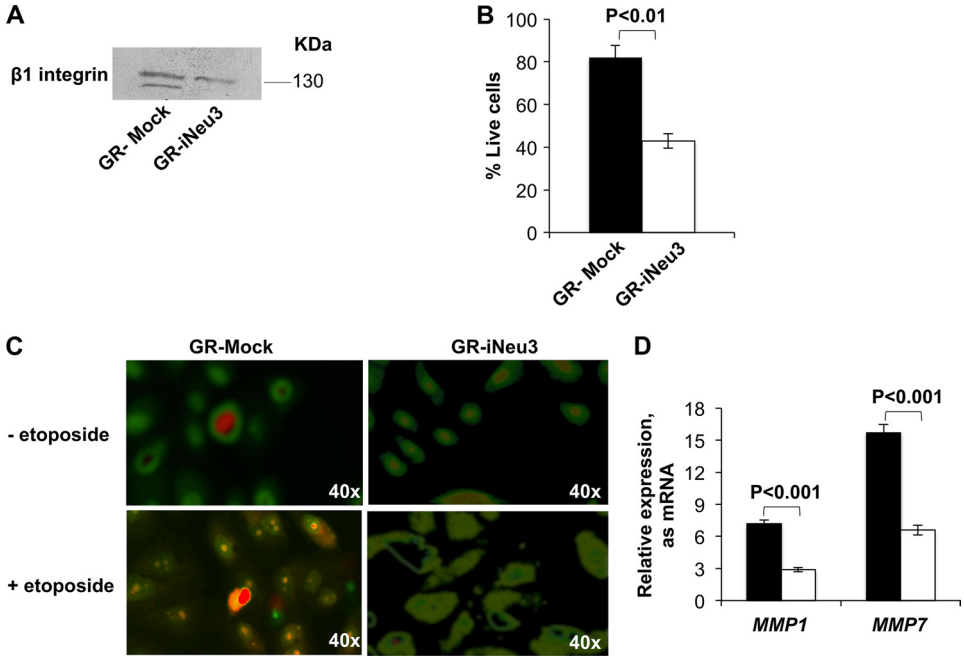

FIGURE 9. **Effect of NEU3 silencing on GR-TC cells.** *A*, Western blot image of GR-mock and GR-iNeu3 cell membrane fractions probed with anti-β1 integrin antibody. An equal amount of proteins was loaded in each lane. Blots are representative of four independent experiments. *B*, GR-mock (*black bar*) and GR-iNeu3 (*white bar*) cell viability assessed through SYTOX staining after etoposide treatment. Values are the mean ± S.D. of three independent experiments. *C*, detection of acidic vesicular organelles in etoposide-treated GR-mock and GR-iNeu3 cells through acridine orange staining. Cells were examined by fluorescence microscope. Representative images from three independent experiments were shown. Original magnification ×40 (Olympus Ix50). *D*, real time PCR analysis of *MMP1* and *MMP7* mRNA expression in GR-mock (*black bar*) and GR-iNeu3 (*white bar*) cells. Values are the mean ± S.D. of three independent experiments.

in MSGG, which suggests the occurrence of an inverse relationship between the synthesis of ganglio-series gangliosides and globo-series gangliosides (37). Therefore, it can be postulated that the increase in gangliosides and the modification of signaling pathways induced by *NEU3* silencing could secondarily affect overall sphingolipid synthesis and further decrease the aggressiveness of RCC cells. Consistent with the molecular events observed, the effects of *NEU3* silencing on the RCC cell malignant phenotype and behavior were significant and involved drug resistance, invasive potential, and adhesion. First, resistance to etoposide decreased. *NEU3* silencing promoted a shift from autophagy, which seemed to be the characteristic response of mock CA-TC cells to etoposide, to apoptosis, which led to the death of *NEU3*-silenced cells. The progression of RCC is usually related to the de-repression of LC3B, which stimulates autophagy and plays a prominent role in sustaining cell viability during nutrient starvation, metabolic stress or radio/chemotherapeutical treatments (38). Possibly, the tendency of *NEU3*-silenced cells to enter apoptosis instead of autophagy relied on changes in *BCL-2* and *BAX* expression. It is well known that *BCL-2* overexpression, as observed in the mock cells, inhibits apoptosis but not autophagy when BCL-2 is targeted to the mitochondria (39). By contrast, *BAX* overexpression, which activates the intrinsic apoptosis pathway, also causes caspase-mediated cleavage of beclin 1 (40). Beclin 1 is the primary inducer of autophagy. After beclin 1 has been cleaved by caspases, it acquires a new apoptosis-promoting function but is not able to activate autophagy (40). The shift of *NEU3*-silenced cells from autophagy to apoptosis was related to a higher rate of cell death in response to etoposide. This is consistent with the observation that autophagy does not necessarily lead to cell death and may act as a protective mechanism in tumor cells treated with chemotherapeutic compounds (41). The second effect that was a consequence of *NEU3* silencing in CA-TC cells was a marked decrease of the adhesion and invasive potential that was caused by the down-regulation of β1 integrin and reduced expression of *MMP1* and *MMP7* that also affected the activity of MMP2 and MMP9. In particular, the increased expression of *MMP7* was previously associated with a poor survival outcome for RCC patients. MMP7 exhibits a wide spectrum of proteolytic activity against many components of the extracellular matrix. It is preferentially expressed at the invasive front of tumors and enhances the infiltrating capability of the tumor by activating MMP2 and MMP9 (42). The *MMP7* and *MMP1* down-regulation that was induced by *NEU3* silencing appeared to be a direct consequence of AKT inhibition because it was reproduced in the mock cells treated with the AKT inhibitor, LY294002. The strong correlation of these events with *NEU3* silencing was demonstrated by the use of clones expressing *NEU3* in different amounts. iNeu3Cl2 and iNeu3Cl3, which displayed 80–90% silencing, demonstrated the same effects, whereas iNeu3Cl1, which displayed only 10% silencing, did not demonstrate any molecular or phenotype changes. Moreover, the main effects observed in CA-TC cells that were a consequence of *NEU3* silencing were also observed in undifferentiated papillary RCC GR-TC cells. Although the global sphingolipid pattern of the GR-TC cells is different from that of CA-TC cells, *NEU3* silencing also induced an increase in GD1a, a decrease in plasma membrane β1 integrin, an increase in cell death after etoposide treatment, and a decrease in *MMP1* and *MMP7* expression in the GR-TC cells.

In conclusion, our results confirmed the primary oncogenic role of *NEU3* up-regulation in RCC and its involvement in β1 integrin trafficking and signaling pathways that are critical for RCC progression. Therefore, NEU3 could be a new molecular target for the development of more specific therapies for RCC.

REFERENCES

1. Cairns, P. (2010) Renal cell carcinoma. *Cancer Biomark* **9,** 461–473
2. Finley, D. S., Pantuck, A. J., and Belldegrun, A. S. (2011) Tumor biology and prognostic factors in renal cell carcinoma. *Oncologist* **16,** Suppl. 2, 4–13
3. Li, L., and Kaelin, W. G., Jr. (2011) New insights into the biology of renal cell carcinoma. *Hematol. Oncol. Clin. North Am.* **25,** 667–686
4. Brenner, W., Greber, I., Gudejko-Thiel, J., Beitz, S., Schneider, E., Walenta, S., Peters, K., Unger, R., and Thüroff, J. W. (2008) Migration of renal carcinoma cells is dependent on protein kinase Cδ via β1 integrin and focal adhesion kinase. *Int. J. Oncol.* **32,** 1125–1131
5. Hoon, D. S., Okun, E., Neuwirth, H., Morton, D. L., and Irie, R. F. (1993) Aberrant expression of gangliosides in human renal cell carcinomas. *J. Urol.* **150,** 2013–2018
6. Senda, M., Ito, A., Tsuchida, A., Hagiwara, T., Kaneda, T., Nakamura, Y., Kasama, K., Kiso, M., Yoshikawa, K., Katagiri, Y., Ono, Y., Ogiso, M., Urano, T., Furukawa, K., Oshima, S., and Furukawa, K. (2007) Identification and expression of a sialyltransferase responsible for the synthesis of disialylgalactosylgloboside in normal and malignant kidney cells: down-regulation of ST6GalNAc VI in renal cancers. *Biochem. J.* **402,** 459–470
7. Biswas, S., Biswas, K., Richmond, A., Ko, J., Ghosh, S., Simmons, M., Rayman, P., Rini, B., Gill, I., Tannenbaum, C. S., and Finke, J. H. (2009) Elevated levels of select gangliosides in T cells from renal cell carcinoma patients is associated with T cell dysfunction. *J. Immunol.* **183,** 5050–5058
8. Aoki, H., Satoh, M., Mitsuzuka, K., Ito, A., Saito, S., Funato, T., Endoh, M., Takahashi, T., and Arai, Y. (2004) Inhibition of motility and invasiveness of renal cell carcinoma induced by short interfering RNA transfection of β1,4GalNAc transferase. *FEBS Lett.* **567,** 203–208
9. Ueno, S., Saito, S., Wada, T., Yamaguchi, K., Satoh, M., Arai, Y., and Miyagi, T. (2006) Plasma membrane-associated sialidase is up-regulated in renal cell carcinoma and promotes interleukin-6-induced apoptosis suppression and cell motility. *J. Biol. Chem.* **281,** 7756–7764
10. Mandal, C., Tringali, C., Mondal, S., Anastasia, L., Chandra, S., Venerando, B., and Mandal, C. (2010) Down regulation of membrane-bound Neu3 constitutes a new potential marker for childhood acute lymphoblastic leukemia and induces apoptosis suppression of neoplastic cells. *Int. J. Cancer* **126,** 337–349
11. Wada, T., Hata, K., Yamaguchi, K., Shiozaki, K., Koseki, K., Moriya, S., and Miyagi, T. (2007) A crucial role of plasma membrane-associated sialidase in the survival of human cancer cells. *Oncogene* **26,** 2483–2490
12. Miyagi, T., Takahashi, K., Hata, K., Shiozaki, K., and Yamaguchi, K. (2012) Sialidase significance for cancer progression. *Glycoconj. J.* **29,** 567–577
13. Tringali, C., Lupo, B., Cirillo, F., Papini, N., Anastasia, L., Lamorte, G., Colombi, P., Bresciani, R., Monti, E., Tettamanti, G., and Venerando, B. (2009) Silencing of membrane-associated sialidase Neu3 diminishes apoptosis resistance and triggers megakaryocytic differentiation of chronic myeloid leukemic cells K562 through the increase of ganglioside GM3. *Cell Death Differ.* **16,** 164–174
14. Monti, E., Bassi, M. T., Papini, N., Riboni, M., Manzoni, M., Venerando, B., Croci, G., Preti, A., Ballabio, A., Tettamanti, G., and Borsani, G. (2000) Identification and expression of NEU3, a novel human sialidase associated to the plasma membrane. *Biochem. J.* **349,** 343–351
15. Anastasia, L., Papini, N., Colazzo, F., Palazzolo, G., Tringali, C., Dileo, L., Piccoli, M., Conforti, E., Sitzia, C., Monti, E., Sampaolesi, M., Tettamanti, G., and Venerando, B. (2008) NEU3 sialidase strictly modulates GM3 levels in skeletal myoblasts C2C12 thus favoring their differentiation and protecting them from apoptosis. *J. Biol. Chem.* **283,** 36265–36271
16. Miyagi, T., Wada, T., Yamaguchi, K., Hata, K., and Shiozaki, K. (2008) Plasma membrane-associated sialidase as a crucial regulator of transmembrane signalling. *J Biochem.* **144,** 279–285
17. Sonnino, S., Nicolini, M., and Chigorno, V. (1996) Preparation of radiolabeled gangliosides. *Glycobiology* **6,** 479–487
18. Steinberg, F., Heesom, K. J., Bass, M. D., and Cullen, P. J. (2012) SNX17 protects integrins from degradation by sorting between lysosomal and recycling pathways. *J. Cell Biol.* **197,** 219–230
19. Papini, N., Anastasia, L., Tringali, C., Croci, G., Bresciani, R., Yamaguchi, K., Miyagi, T., Preti, A., Prinetti, A., Prioni, S., Sonnino, S., Tettamanti, G., Venerando, B., and Monti, E. (2004) The plasma membrane-associated sialidase MmNEU3 modifies the ganglioside pattern of adjacent cells supporting its involvement in cell-to-cell interactions. *J. Biol. Chem.* **279,** 16989–16995
20. Sonnino, S., and Prinetti, A. (2010) Gangliosides as regulators of cell membrane organization and functions. *Adv. Exp. Med. Biol.* **688,** 165–184
21. Hua, H., Li, M., Luo, T., Yin, Y., and Jiang, Y. (2011) Matrix metalloproteinases in tumorigenesis: an evolving paradigm. *Cell Mol. Life Sci.* **68,** 3853–3868
22. Wang, F., Reierstad, S., and Fishman, D. A. (2006) Matrilysin over-expression in MCF-7 cells enhances cellular invasiveness and pro-gelatinase activation. *Cancer Lett* **236,** 292–301
23. Mosesson, Y., Mills, G. B., and Yarden, Y. (2008) Derailed endocytosis: an emerging feature of cancer. *Nat. Rev. Cancer* **8,** 835–850
24. Sonnino, S., and Prinetti, A. (2009) Sphingolipids and membrane environments for caveolin. *FEBS Lett.* **583,** 597–606
25. Dozynkiewicz, M. A., Jamieson, N. B., Macpherson, I., Grindlay, J., van den Berghe, P. V., von Thun, A., Morton, J. P., Gourley, C., Timpson, P., Nixon, C., McKay, C. J., Carter, R., Strachan, D., Anderson, K., Sansom, O. J., Caswell, P. T., and Norman, J. C. (2012) Rab25 and CLIC3 collaborate to promote integrin recycling from late endosomes/lysosomes and drive cancer progression. *Dev. Cell* **22,** 131–145
26. Wang, S., and Basson, M. D. (2011) Protein kinase B/AKT and focal adhesion kinase: two close signaling partners in cancer. *Anticancer Agents Med. Chem.* **11,** 993–1002
27. Streuli, C. H., and Akhtar, N. (2009) Signal co-operation between integrins and other receptor systems. *Biochem. J.* **418,** 491–506
28. Banumathy, G., and Cairns, P. (2010) Signaling pathways in renal cell carcinoma. *Cancer Biol. Ther.* **10,** 658–664
29. Azim, H., Azim, H. A., Jr., and Escudier, B. (2010) Targeting mTOR in cancer: renal cell is just a beginning. *Target Oncol.* **5,** 269–280
30. Wang, Y., Yamaguchi, K., Wada, T., Hata, K., Zhao, X., Fujimoto, T., and Miyagi, T. (2002) A close association of the ganglioside-specific sialidase Neu3 with caveolin in membrane microdomains. *J. Biol. Chem.* **277,** 26252–26259
31. Rathinam, R., and Alahari, S. K. (2010) Important role of integrins in the cancer biology. *Cancer Metastasis Rev.* **29,** 223–237
32. Schwartz, M. A., and Ginsberg, M. H. (2002) Networks and crosstalk: integrin signalling spreads. *Nat. Cell Biol.* **4,** E65–68
33. Singh, R. D., Marks, D. L., Holicky, E. L., Wheatley, C. L., Kaptzan, T., Sato, S. B., Kobayashi, T., Ling, K., and Pagano, R. E. (2010) Gangliosides and β1-integrin are required for caveolae and membrane domains. *Traffic* **11,** 348–360
34. Park, S. Y., Kwak, C. Y., Shayman, J. A., and Kim, J. H. (2012) Globoside promotes activation of ERK by interaction with the epidermal growth factor receptor. *Biochim. Biophys. Acta* **1820,** 1141–1148
35. Zhao, J., and Guan, J. L. (2009) Signal transduction by focal adhesion kinase in cancer. *Cancer Metastasis Rev.* **28,** 35–49
36. Saito, S., Orikasa, S., Satoh, M., Ohyama, C., Ito, A., and Takahashi, T. (1997) Expression of globo-series gangliosides in human renal cell carcinoma. *Jpn. J. Cancer Res.* **88,** 652–659
37. Saito, S., Nojiri, H., Satoh, M., Ito, A., Ohyama, C., and Orikasa, S. (2000) Inverse relationship of expression between GM3 and globo-series ganglioside in human renal cell carcinoma. *Tohoku J. Exp. Med.* **190,** 271–278
38. Mikhaylova, O., Stratton, Y., Hall, D., Kellner, E., Ehmer, B., Drew, A. F., Gallo, C. A., Plas, D. R., Biesiada, J., Meller, J., and Czyzyk-Krzeska, M. F. (2012) VHL-regulated MiR-204 suppresses tumor growth through inhibition of LC3B-mediated autophagy in renal clear cell carcinoma. *Cancer Cell* **21,** 532–546
39. Hetz, C., and Glimcher, L. (2008) The daily job of night killers: alternative roles of the BCL-2 family in organelle physiology. *Trends Cell Biol.* **18,** 38–44

40. Djavaheri-Mergny, M., Maiuri, M. C., and Kroemer, G. (2010) Cross talk between apoptosis and autophagy by caspase-mediated cleavage of Beclin 1. *Oncogene* **29,** 1717–1719
41. Liang, X., De Vera, M. E., Buchser, W. J., Romo de Vivar Chavez, A., Loughran, P., Beer Stolz, D., Basse, P., Wang, T., Van Houten, B., Zeh, H. J., 3rd, and Lotze, M. T. (2012) Inhibiting Systemic Autophagy during Interleukin 2 Immunotherapy Promotes Long-term Tumor Regression. *Cancer Res.* **72,** 2791–2801
42. Ramankulov, A., Lein, M., Johannsen, M., Schrader, M., Miller, K., and Jung, K. (2008) Plasma matrix metalloproteinase-7 as a metastatic marker and survival predictor in patients with renal cell carcinomas. *Cancer Sci.* **99,** 1188–1194